Active rod-like particles suspension in non-homogenoeus system: The effect of active motion and flow/rod coupling

Hamza Issa, Giovanniantonio Natale, Gilles Ausias, Julien Férec

Active rod-like particles suspension in non-homogenoeus system: The effect of active motion and flow/rod coupling

Hamza Issa
Univ. Bretagne Sud, UMR CNRS 6027, IRDL, F-56100 Lorient, France
Department of Chemical and Petroleum Engineering, Schulich School of Engineering, University of Calgary, 2500 University Drive NW, T2N 1N4, Canada

Giovanniantonio Natale
Department of Chemical and Petroleum Engineering, Schulich School of Engineering, University of Calgary, 2500 University Dr. NW, T2N 1N4, Canada

Gilles Ausias
Univ. Bretagne Sud, UMR CNRS 6027, IRDL, F-56100 Lorient, France

Julien Férec
Univ. Bretagne Sud, UMR CNRS 6027, IRDL, F-56100 Lorient, France
(Dated: November 26, 2024)

This study explores active Brownian rods in simple shear flow, examining the influence of self-propulsion (Pe_s), rotary diffusion (Pe_r), and translational diffusion ($Pe_\perp$). We observe these rods accumulating near walls, aligning with the flow direction, with more pronounced effects at higher Pe_s and $Pe_\perp$, and lower Pe_r. Furthermore, we examine the impact of particle extra stress in simple shear flows, observing shear banding and rheological changes. These findings enhance our understanding of complex effect created by active particles.

I. INTRODUCTION

Several biological processes depend on the mobility of active self-propelled particles and their interactions with solid boundaries. Numerous studies have looked into the mobility of biological particles in confined spaces experimentally [1–4] and numerically [5–7]. The accumulation of active particles on channel walls has been observed. In their additional analysis of the hydrodynamic interactions, Kaya and Koser [8] demonstrated that Escherichia coli cells undergo modified Jeffery orbits near walls [9]. Understanding the upstream migration phenomenon requires knowing this specific information. A greater understanding of this phenomena was offered by more recent study by Kaya and Koser [10], who carefully investigated Escherichia coli motility near a surface as a function of the local shear rate. Swimming dynamics and near-wall aggregation have been the main topics of most confinement-based experimental research. To explain how collective motion emerged in semi-dilute suspensions, Saintillan and Shelley developed a group of models [11, 12] to explain how collective motion emerged in semi-dilute suspensions.In these models, the particle positions and orientations are represented by a distribution function that is based on a conservation equation.The fluxes brought on by diffusive, advective, rotating, and self-propelled processes are all taken into consideration by these models. They examined the stability of aligned suspensions and showed that they are consistently unstable to fluctuations, a finding that confirms earlier hypotheses by Simha and Ramaswamy [13]. They also demonstrated that an instability for the particle stress occurs when isotropic suspensions are taken into account. An active particle impose a net force dipole on the surrounding fluid [5, 12] as it moves forward due to the balance between the propulsive force and viscous drag on its body. This force dipole can take either a positive or a negative sign depending on how the particle drives itself through the fluid: a pusher particle will produce a negative dipole while a puller particle will produce a positive dipole. Hatwalne et al. [14], who generalized liquid crystal kinetic equations to represent the rheology of active suspensions, discovered that for pushers the effective viscosity would decrease and for pullers it would increase. Ishikawa and Pedley [15] then carried out simulations of Stokesian dynamics of suspensions of spherical 'squirmers' that swim as a result of a specified slip velocity on their surface. They discovered that swimming had no influence on effective viscosity in the dilute limit. A result of the spherical shape, which generates an isotropic distribution of orientation. Haines et al. [16] demonstrated through analytical calculations that swimming does definitely cause a change in viscosity if the orientation distribution is considered to be anisotropic. Additionally, they saw a reduction in the viscosity of pusher suspensions. Saintillan [17] discovered that tail-actuated swimmers significantly reduce the fluid's effective shear viscosity and that the rheology is characterized by much higher normal stress differences than for passive suspensions. Recent research has found that bacterial suspensions exhibit counter-intuitive behavior when subjected to external shear, including regimes of apparent superfluidity [18, 19]. By demonstrating a novel concentration-shear coupled mechanism, Vennamneni et al. [20] show how fluctuations in bacterial suspensions can grow and eventually reach

banded steady states. In stark contrast to the passive complex fluids [21–23] and active fluids [24, 25] studied earlier, the proposed mechanism is shown to result in shear bands, with concentration inhomogeneities, in the dilute regime. Previously, shear banding was only observed or predicted in the semi-dilute and concentrated regimes.
Here we explore the effect of the active particles extra stress contribution in the simple shear flow. After the introduction, the theoretical modeling and the flow problem for active rods are derived in Sec. II. Then, before conclusion Sec. III presents the numerical results in simple shear flow including the effects of rotary and translational Peclet numbers, in addition to the effect of extra stress generated by active particles.

II. HYPOTHESIS

Consider a suspension of active particles that resemble Brownian rods and have length L and width d. The active rods are rigid, neutrally buoyant, and mono-dispersed. The suspension is taken into account in the regime of diluted concentration. Active rods are polar, meaning that their heads and tails aren't exactly the same. Each rod is described by a position vector $\mathbf{r}_c$ and an orientation unit vector $\mathbf{p}$.

A. Kinetic model equation

A probability distribution function $\Psi(\mathbf{r}_c, \mathbf{p}, t)$ can be used to characterize a suspension of active Brownian particles. It represents the probability that particles will be present at position $\mathbf{r}_c$ and orientation $\mathbf{p}$ at time t. A single-particle Smoluchowski equation can be derived in a diluted state as

$$\frac{\partial \Psi}{\partial t} = -\nabla_{\mathbf{x}} \cdot (\dot{\mathbf{r}}_c \Psi) - \nabla_{\mathbf{p}} \cdot (\dot{\mathbf{p}} \Psi) \,. \tag{1}$$

The evolution of the position of an active Brownian particle with respect to time , $\dot{\mathbf{r}}_c$, is [11]

$$\dot{\mathbf{r}}_c = \mathbf{u} + V_s \mathbf{p} - \mathbf{D}_t \cdot \nabla_{\mathbf{x}} \log \Psi, \tag{2}$$

where V_s is the particle velocity. The evolution of its orientation with respect to time, $\dot{\mathbf{p}}$, can be written as

$$\dot{\mathbf{p}} = \dot{\mathbf{p}}_j - D_r \nabla_{\mathbf{p}} \log \Psi, \tag{3}$$

where $\dot{\mathbf{p}}_j$ is the Jeffery's equation and it is given by [9]

$$\dot{\mathbf{p}}_j = -\frac{1}{2} \boldsymbol{\omega} \cdot \mathbf{p} + \frac{\lambda}{2} \left(\dot{\boldsymbol{\gamma}} \cdot \mathbf{p} - \dot{\boldsymbol{\gamma}} : \mathbf{ppp} \right). \tag{4}$$

D_r and $\mathbf{D}_t$ are the rotary diffusion coefficient and translational diffusion tensor , respectively. The latter for non-spherical, rigid particles is defined by $\mathbf{D}_t = D_{\parallel} \mathbf{pp} + D_{\perp} (\boldsymbol{\delta} - \mathbf{pp})$, where $D_{\parallel}$ and $D_{\perp}$ are constants that characterize the diffusion parallel and perpendicular to the particle axis [26]. $\mathbf{u}$ is the external flow velocity vector at location $\mathbf{r}_c$. $\nabla_{\mathbf{p}}$ and $\nabla_{\mathbf{x}}$ denote the gradient operators in configurational and spatial spaces, respectively. $\boldsymbol{\omega}$, $\dot{\boldsymbol{\gamma}}$, and $\boldsymbol{\delta}$ are the vorticity, strain rate, and identity tensors, respectively. λ is a constant form factor as a function of the particle aspect ratio $a_r = L/d$, in the case of rods, $\lambda = 1$. Hence, the expanded version of Eq. 1, by taking into account the fluid incompressibility condition, is

$$\frac{D\Psi}{Dt} = -\nabla_{\mathbf{x}} \cdot (V_s \mathbf{p} \Psi) + \nabla_{\mathbf{x}} \cdot (\mathbf{D}_t \cdot \nabla_{\mathbf{x}} \Psi) - \nabla_{\mathbf{p}} \cdot (\dot{\mathbf{p}}_j \Psi) + D_r \nabla_{\mathbf{p}}^2 \Psi, \tag{5}$$

where $\frac{D(...)}{Dt} = \frac{\partial (...)}{\partial t} + \mathbf{u} \cdot \nabla_{\mathbf{x}} (...)$ is the material derivative operator, and $\nabla_{\mathbf{p}}^2$ is the Laplacian operator in configurational domain. In what follows, we derive an equivalent evolution equation based on the second-order moment of Ψ.

B. Flow problem

The problem is governed by the continuity and Cauchy momentum equations in the limit of creeping flow

$$\nabla_{\mathbf{x}} \cdot \mathbf{u} = 0, \tag{6}$$

$$-\eta_0 \nabla_{\mathbf{x}}^2 \mathbf{u} + \nabla_{\mathbf{x}} P = \nabla_{\mathbf{x}} \cdot \boldsymbol{\Sigma}. \tag{7}$$

In the above equations, $\nabla_{\mathbf{x}}^2$ is the Laplacian operator in the spatial space, η_0 is the dynamic viscosity of the Newtonian suspending fluid, P denotes the pressure and $\boldsymbol{\Sigma}$ represents the extra stress tensor. Indeed, the presence of active particles in a Newtonian medium develops extra stress contributions, which are obtained by configurational averages of force dipoles exerted by the particle on the fluid. In the case of interest, the dipole arises from several contributions, including hydrodynamic stress, Brownian stresses, and the permanent dipole due to self-propulsion. The extra stress is calculated following the work of saintillan et al. [17].

$$\boldsymbol{\Sigma} = \boldsymbol{\Sigma}_s + \boldsymbol{\Sigma}_B + \boldsymbol{\Sigma}_F. \tag{8}$$

The first contribution is resulting from the particle swimming and can be expressed as

$$\boldsymbol{\Sigma}_s = \sigma_0(\mathbf{A}_2 - \mathbf{A}_2 : \boldsymbol{\delta}\boldsymbol{\delta}/3), \tag{9}$$

where σ_0 is the dipole or stresslet strength, which depends on the swimming mechanism. It is a constant and can be used to measure the particle activity. It should be noted that depending on the type of swimmer, σ_0 can be either positive or negative. For example, it can be demonstrated that $\sigma_0 < 0$ for most swimming bacteria (such as Escherichia coli and Bacillus subtilis) and $\sigma_0 > 0$ for head-actuated swimmers or pullers, such as the alga Chlamydomonas Reinhardtii [11].
The second contribution is due to the fact that particles are Brownian. It is

$$\boldsymbol{\Sigma}_B = k_B T(3\mathbf{A}_2 - \mathbf{A}_2 : \boldsymbol{\delta}\boldsymbol{\delta}), \tag{10}$$

where k_B and T are the Boltzmann constant and the absolute temperature, respectively. The third contribution comes from the inextensibility of the particles and is expressed as

$$\boldsymbol{\Sigma}_F = \sigma_F \left[(\mathbf{A}_4 - \boldsymbol{\delta}\mathbf{A}_2/3) : \dot{\boldsymbol{\gamma}}\right], \tag{11}$$

where $\sigma_F = \pi\eta_0/6 \log(2a_r)$ from slender body theory.
Substituting Eqs. 9, 10 and 11 into Eq. 8 gives the detailed expression of the particle extra stress

$$\boldsymbol{\Sigma} = (\sigma_0 + 3k_B T)(\mathbf{A}_2 - \mathbf{A}_2 : \boldsymbol{\delta}\boldsymbol{\delta}/3) + \sigma_F \left[(\mathbf{A}_4 - \boldsymbol{\delta}\mathbf{A}_2/3) : \dot{\boldsymbol{\gamma}}\right] \tag{12}$$

C. Dimensionless formulation of the problem

Choosing the active rod length L as the characteristic length and the characteristic strain rate $\dot{\gamma} = U_{avg}/L$, where U_{avg} is the average flow velocity, and the dimensionless concentration $c^* = \frac{c}{n}$, where n is the mean number number density. The dimensionless form of FP equation (Eq. 5) is

$$\frac{D\Psi}{D\tau} = -Pe_s \nabla_{\mathbf{x}}^* \cdot (\mathbf{p}\Psi) + \nabla_{\mathbf{x}}^* \cdot \left\{ \left[\frac{1}{Pe_{\parallel}} \mathbf{pp} + \frac{1}{Pe_{\perp}} (\boldsymbol{\delta} - \mathbf{pp}) \right] \cdot \nabla_{\mathbf{x}}^* \Psi \right\} - \nabla_{\mathbf{p}} \cdot (\dot{\mathbf{p}_j} \Psi) + \frac{1}{Pe_r} \nabla_{\mathbf{p}}^2 \Psi, \tag{13}$$

where the dimensionless number $Pe_s = \frac{Vs}{L\dot{\gamma}}$ denotes the active rod's relative velocity to the flow velocity. This dimensionless value can shed light on how active rods react to the shear flow that is being applied.
The dimensionless of the continuity equation is

$$\nabla_{\mathbf{x}}^* \cdot \mathbf{u}^* = 0, \tag{14}$$

The dimensionless form of the Cauchy equation can be written as

$$\nabla_{\mathbf{x}}^* P^* - \nabla_{\mathbf{x}}^{*2} \mathbf{u}^* = \nabla_{\mathbf{x}}^* \cdot \left\{ c^* \left[N_p \left(\mathbf{A}_4^* - \frac{1}{3}\boldsymbol{\delta}\mathbf{A}_2^* \right) : \dot{\boldsymbol{\gamma}}^* + (N_b + N_s)(3\mathbf{A}_2^* - \boldsymbol{\delta}) \right] \right\}. \tag{15}$$

As a result, the dimensionless form of the stress tensor is

$$\boldsymbol{\Sigma}^* = c^* \left[N_p \left(\mathbf{A}_4 - \frac{1}{3}\boldsymbol{\delta}\mathbf{A}_2 \right) : \dot{\boldsymbol{\gamma}}^* + (N_b + N_s)(3\mathbf{A}_2^* - \boldsymbol{\delta}) \right], \tag{16}$$

where $N_p = \frac{\pi n L^3}{6log(a_r)}$ is the particle coupling coefficient, $N_b = \frac{n k_B T}{\eta_0 \dot{\gamma}}$ is the Brownian coupling coefficient and $N_s = \frac{n\sigma_0}{\eta_0 \dot{\gamma}}$ is the self propulsion coupling coefficient.

III. NUMERICAL RESULTS

We employ the finite volume method to investigate two flow problems, solving the problem defined in Eqs. 13, 14 and 15 . The indices 1 and 2 represent the flow direction and the velocity gradient direction, respectively. In a simple shear flow and Poiseuille flow, they are indicated with x and y, respectively.

A. Simple shear flow

A squared 2D channel with side length H undergoes a simple shear flow between opposing moving walls. Here, the aspect ratio is defined as $H/L = 10^6$. To emulate an infinite flow channel, periodic flow conditions with $\Delta P = 0$ are employed (refer to Fig. 1). The initial conditions for the conformation tensor are set as $A_{ii} = 1/3$ and $A_{ij} = 0$ for $i \neq j$. The initial concentration is homogeneous and equals to one.

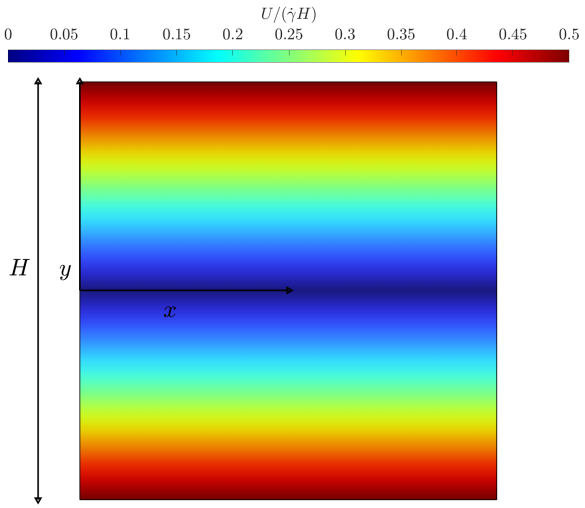

FIG. 1: Dimensionless velocity magnitude in the squared channel, of side H, for simple shear flow with periodic BC.

1. *Effect of self-propulsion*

We examine three distinct regimes based on the active rods self propulsion Peclet number (Pe_s) and the diffusion Peclet numbers (Pe_r and $Pe_\perp$). The first regime ($Pe_s < Pe_r, Pe_\perp$) explores scenarios where the directed motion due to self-propulsion is relatively weak. The second regime ($Pe_s = Pe_r = Pe_\perp$) corresponds to cases where there is a competition between active motion and diffusion. Lastly, the third regime ($Pe_s > Pe_r, Pe_\perp$), investigates situations where active motion dominates over diffusion. The Peclet numbers in this case are fixed to $Pe_\perp = Pe_r = 10$ while the value of Pe_s equals $0, 5, 10$ and 15. In this section, no active rods extra stresses is taken into consideration and the flow problem is developed from Eq. 15.
In simple shear flows, active rods exhibit significant transverse migration, a behavior distinct from that of Brownian-passive rods ($Pe_s = 0$). Notable aggregation of active rods near the mobile walls is observed (see Fig. 2a). The intensity of active rod clustering in regions of higher flow velocity correlates directly with the magnitude of the self-propulsion Peclet number. As depicted in Fig.2b, an increase in the self-propulsion Peclet number (Pe_s) prompts enhanced alignment of active rods along the flow direction at the center of the channel. Conversely, active rods near the channel walls display diminished alignment. This observation highlights the correlation between selfpropulsion velocity and alignment dynamics, illustrating a tendency for stronger alignment in regions of low concentration and weaker alignment towards the high concentration regions. Figure 2c illustrates that A_{12}/c exhibits a positive value near the walls and a negative value at the channel center. Conversely, Figure 2d indicates that n_2/c shares the same sign as y/H, with its maximum absolute values observed at the walls and zero at the center. This observation suggests that near the walls, active rods align with the flow direction while displaying nematic order oriented towards

the walls. In contrast, at the channel center, active rods align opposite to the flow direction, also displaying nematic order towards the walls.

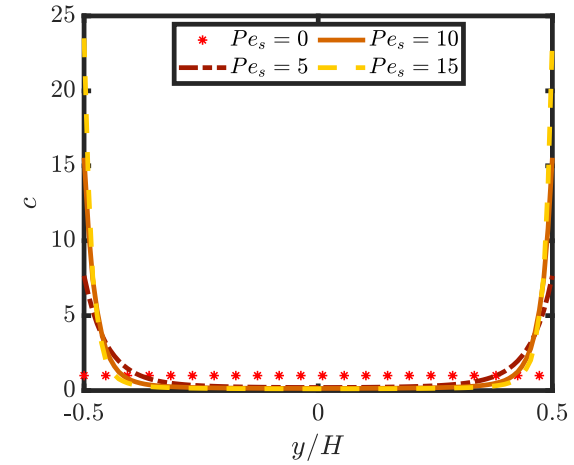

(a) Effect of the The self-propulsion Peclet number, Pe_s, on the concentration distribution, c, along the y direction.

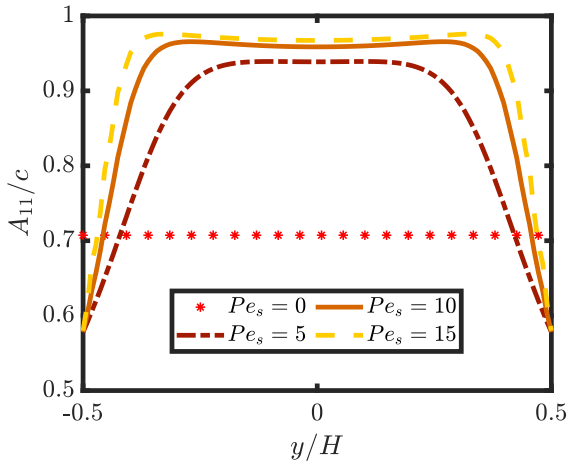

(b) Effect of the self-propulsion Peclet number, Pe_s, on the orientation component, A_{11}/c, along the y direction.

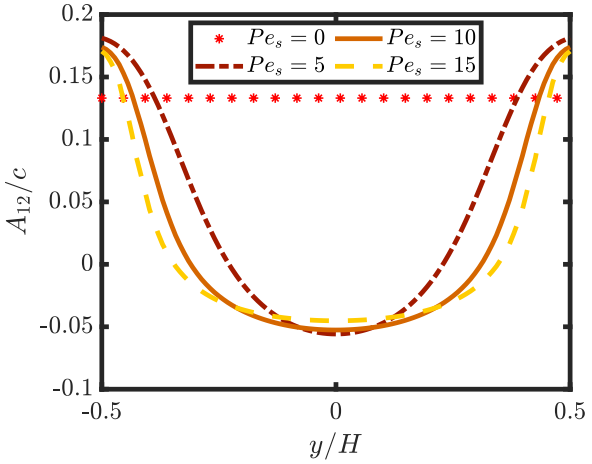

(c) Effect of the self-propulsion Peclet number, Pe_s, on the orientation component, A_{12}/c, along the y direction

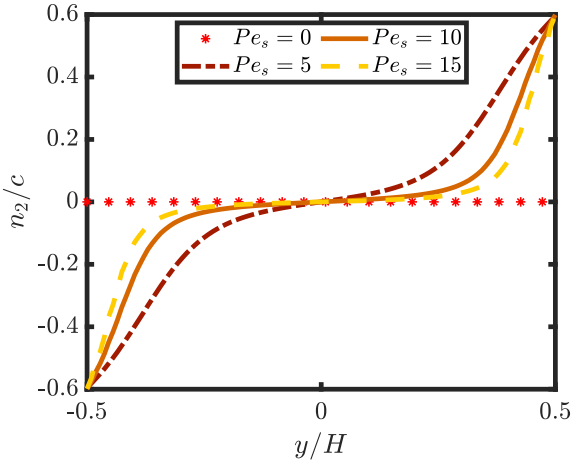

(d) Effect of the self-propulsion Peclet number, Pe_s, on the nematic order, n_2/c, along the y direction.

FIG. 2: Showing the effect of the self-propulsion Peclet number, $Pe_s = 0, 5, 10$ and 15,(a) on the concentration distribution, c, (b) on the orientation component, A_{11}/c, (c) on the orientation component, A_{12}/c, (d) on the nematic order, n_2/c, along the y direction at steady state, in simple shear flow.

2. Effect of rotary diffusion

With fixed values of $Pe_s = 5$ and $Pe_\perp = 10$, we focus on the impact of rotary diffusion on the migration behavior of active rods. As shown in Fig. 3a, a decrease in the rotary Peclet number (Pe_r) corresponds to a stronger tendency for active rods to accumulate at the walls. This observation implies that, even in the case of active rods, isotropic active rods have more tendency to migrate across streamlines than the aligned ones [27]. Fig. 3b demonstrates that active rods display a nematic ordering directed toward the walls, with varying degrees of alignment corresponding to different rotary Peclet values. Remarkably, as the rotary Peclet number (Pe_r) decreases, the nematic order (n_2) becomes increasingly prominent.

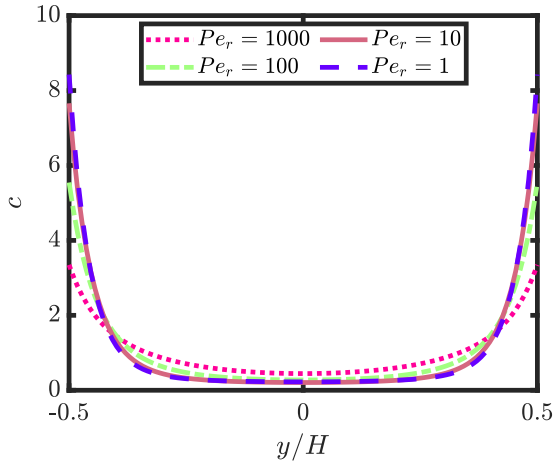

(a) Effect of the rotary diffusion, Pe_r, on the concentration distribution, c, along the y direction.

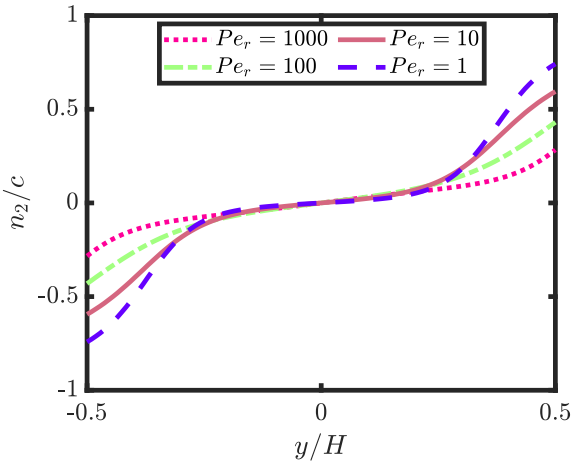

(b) Effect of the rotary diffusion, Pe_r, on the nematic order, n_2/c, along the y direction.

FIG. 3: Showing the effect of the rotary diffusion, $Pe_r = 1, 10, 100$ and 1000, (a) on the concentration distribution, c, (b) on the nematic order, n_2/c, along the y direction at steady state, in simple shear flow.

3. Effect of translational diffusion

For passive rods subjected to simple shear flow, translational diffusion exerts negligible influence on both rod migration and orientation. However, distinct behaviors emerge for active rods experiencing simple shear flows. To elucidate the influence of translational Peclet numbers on the system, other Peclet numbers are held constant at $Pe_r = 10$ and $Pe_s = 5$. At higher translational Peclet numbers, active rods tend to aggregate near the walls, whereas as the translational Peclet number decreases, the distribution of active rods becomes more uniform along the channel (refer to Fig. 4a). Regarding active rod orientations, under high Peclet numbers, active rods predominantly align in the flow direction at the channel center, while exhibiting a nearly isotropic arrangement near the high-concentration walls. A decrease in the Peclet number results in a diminished gradient of active rod orientation along the y direction, as shown in Fig. 4b. For active rods, when self-propulsion predominates at high $Pe_\perp$, there is an accumulation of active rods near the walls, accompanied by a high degree of alignment in the flow direction. As $Pe_\perp$ decreases further, translational diffusion becomes dominant, leading the system back to a homogeneous state. Figs. 4c and 4d shows that active rods exhibit a distinct orientation toward the walls within the vicinity of the walls. However, as one moves towards the center of the channel, the orientation of active rods is more randomized. As translational diffusion exerts a growing influence, active rods appear to lose any preferential alignment along the flow direction. This transition towards a more uniform distribution of active rod orientations underscores the counteractive role of diffusion against alignment tendencies induced by the active flow.

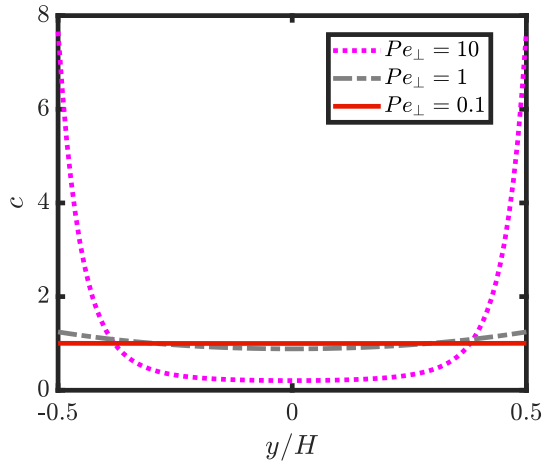

(a) Effect of the translational diffusion, $Pe_\perp$, on the concentration distribution, c, along the y direction.

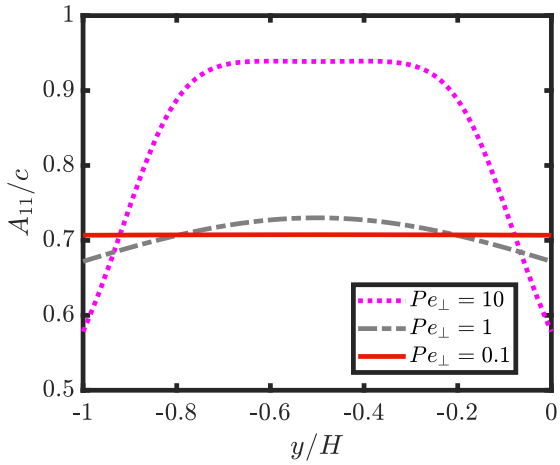

(b) Effect of the translational diffusion, $Pe_\perp$, on the orientation component, A_{11}/c, along the y direction.

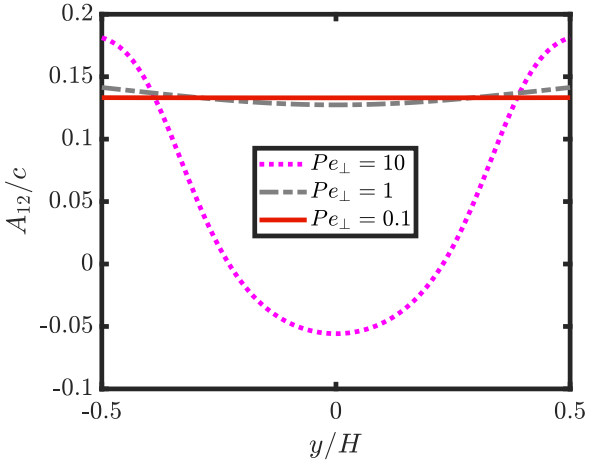

(c) Effect of the translational diffusion, $Pe_\perp$, on the orientation component, A_{12}/c, along the y direction.

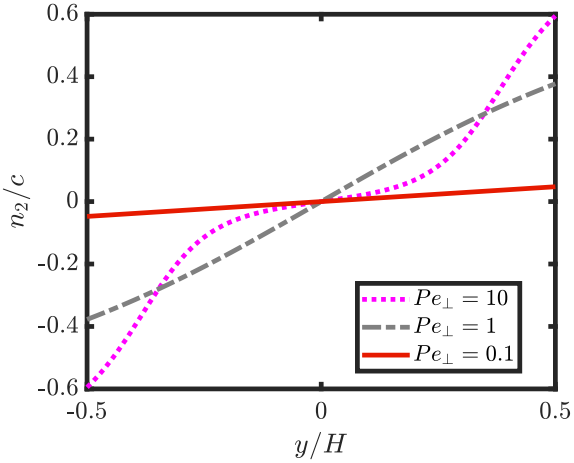

(d) Effect of the translational diffusion, $Pe_\perp$, on the nematic order, n_2/c, along the y direction.

FIG. 4: Showing the effect of the translational diffusion, $Pe_\perp = 0.1, 1$ and 10, (a) on the concentration distribution, c, (b) on the orientation component, A_{11}/c, (c) on the orientation component, A_{11}/c, (d) the nematic order, n_2/c, along the y direction at steady state, in simple shear flow.

4. Effect of particles extra stress

We conducted an investigation into the influence of particle stress within a simple shear flow context. Specifically, we maintained fixed Peclet numbers of $Pe_r = Pe_\perp = 10$ and a constant coupling coefficient of $N_p = 0$. Our study involved examining values of Pe_s ranging from 0 to 15. Unlike scenarios involving passive rods, where particle stress has minimal effect on the simple shear flow, our findings revealed distinct alterations in the behavior of active particles in response to such stress. Our focus lies in comprehensively exploring the impact of Pe_s on the rheological dynamics exhibited by the system.

- Pusher rods

  For pusher active rods, the additional stress induced by the rod is positive, denoted by $N_b + N_s = 10$. The behavior is elucidated in Fig. 5, which showcases variations in velocity profiles at steady state for different Pe_s values. Analyzing solely one half of the simple shear flow profile, the findings reveal the occurrence of a reverse flow directed opposite to the moving wall. The system predicts shear banding, indicative of shear deformation.

These results align well with the observations of Vennamneni et al. [20], who noted shear bands accompanied by concentration inhomogeneities in the dilute regime.

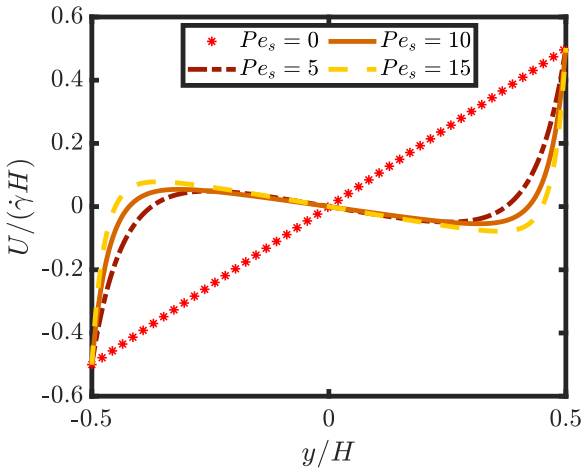

FIG. 5: Effect of the self-propulsion Peclet number, Pe_s, on the velocity profile at steady state, initially simple shear flow, for $N_b = 10$.

Figure 6a elucidates the influence of the self-propulsion Peclet number on the evolution of shear viscosity concerning strain. Notably, the outcomes highlight a direct correspondence between shear viscosity values and Pe_s. The decline in shear viscosity with increasing Pe_s is attributed to intricate interactions between active rods and the surrounding fluid. Consequently, pushers tend to reduce suspension viscosity.

Figure 6b demonstrates the effect of the self-propulsion Peclet number on the evolution of normal stress differences concerning deformation at the moving wall. With increasing self-propulsion Peclet number (Pe_s), the values of normal stress differences also rise. As Pe_s increases, so does the intensity of self-propulsion, leading to heightened activity and more robust active rod-fluid interactions. Consequently, the suspension exhibits greater resistance to deformation. Essentially, the energetic motion of active rods contributes to increased resistance to flow, resulting in elevated viscosity values and heightened stress contributions. In this context, the orientation and concentration distributions qualitatively resemble the findings in Section III A 1.

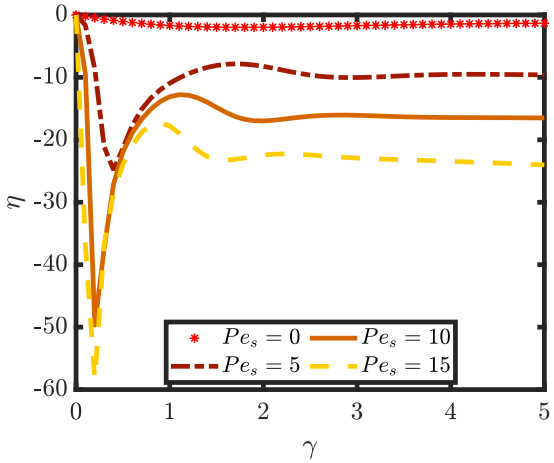

(a) Effect of self-propulsion Peclet number, Pe_s, on the evolution of the shear viscosity with respect to deformation.

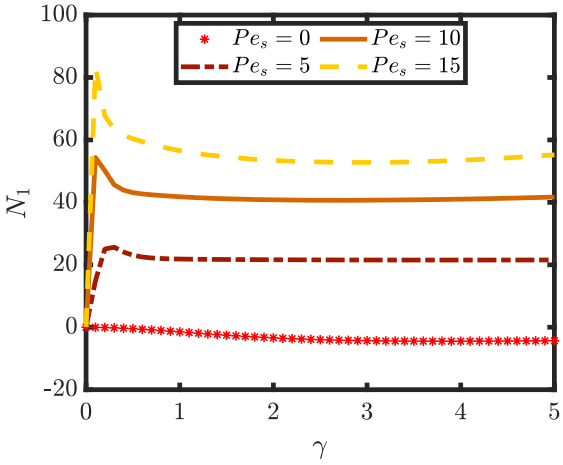

(b) Effect of self-propulsion Peclet number, Pe_s, on the evolution of the normal stresses difference with respect to deformation.

FIG. 6: Showing the effect of the self-propulsion Peclet number, Pe_s, on the rheological properties (a) shear viscosity, η, (b) the normal stress differences, N_1, with respect to the deformation, γ, in simple shear flow.

- Puller rods

  For puller active rods, the additional stress induced by the rod is negative, denoted by $N_b+N_s = -10$. Illustrated in Fig. 7, is the influence of particle extra stress and varying Pe_s values on the velocity profiles at steady state. The figure demonstrates a slight deviation from the conventional linear profile observed in standard simple shear flow. Notably, higher Pe_s values correspond to accelerated flow rates. Moreover, it depicts shear banding, contrary to the case of pushers, with less deformation.

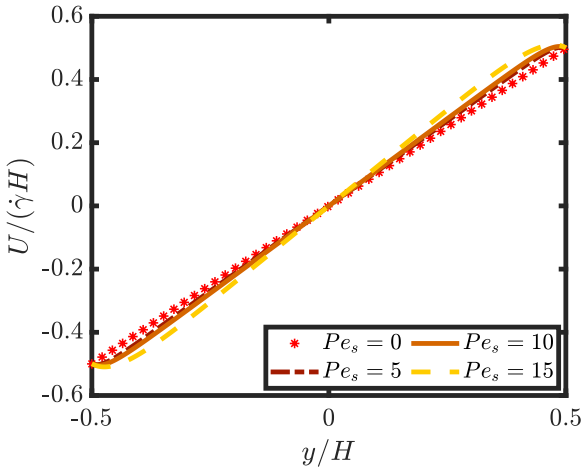

FIG. 7: Effect of self-propulsion Peclet number, Pe_s, on the velocity profile at steady state, initially simple shear flow, for $N_b = 10$.

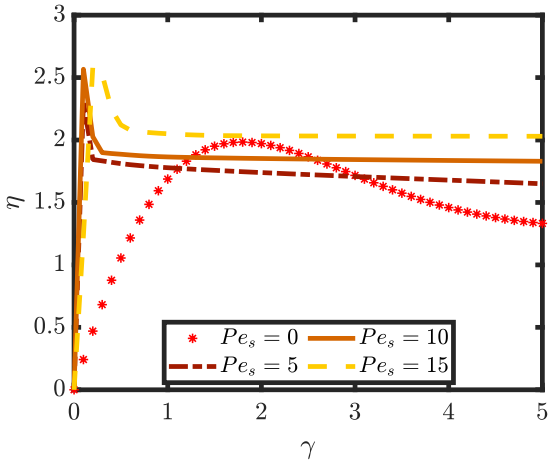

(a) Effect of self-propulsion Peclet number, Pe_s, on the evolution of the shear viscosity with respect to deformation.

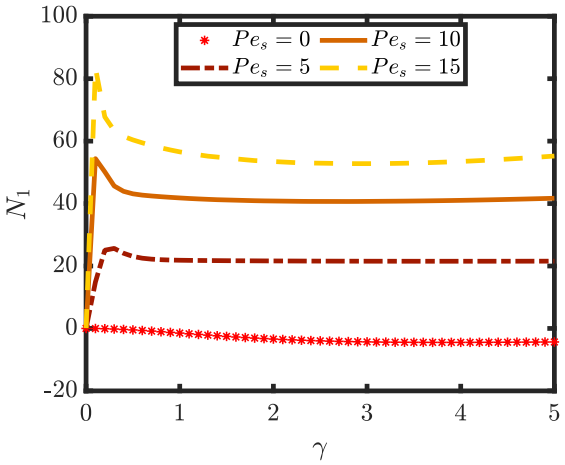

(b) Effect of self-propulsion Peclet number, Pe_s, on the evolution of the normal stresses difference with respect to deformation.

FIG. 8: Showing the effect of the self-propulsion Peclet number, Pe_s, on the rheological properties (a) shear viscosity, η, (b) the normal stress differences, N_1, with respect to the deformation, γ, in simple shear flow.

In the case of puller active rods, the presence of active suspension leads to an increase in the shear viscosity of the suspended flow, as depicted in Fig. 8a. Additionally, there is a concurrent increase in the normal stress differences, as illustrated in Fig. 8b. These findings corroborate the observations of Matilla et al. [28], who reported that pushers tend to decrease suspension viscosity while pullers enhance it.

For both pusher and puller active rods, the influence of Pe_s on concentration, orientation, and nematic order align

qualitatively with those discussed in Section III A 1. Specifically, with increasing Pe_s, active rods tend to accumulate more near the walls and align more strongly in the flow direction, with nematic order towards the walls.

IV. CONCLUSION

In conclusion, this work explores the rheology of active rod suspensions in simple shear flow, including simple shear flow. The study examines the dynamics of active rods including active rod migrations, orientations and the nematic order in addition to effect of active rod-fluid coupling in simple shear flow, through numerical simulations based on the volume method with taking into consideration an anisotropic translational diffusion.
The active rods are more aligned with the flow direction than the passive rods, favoring accumulation near the channel walls. However, compared to aligned active rods, randomly aligned active rods with low rotational Peclet numbers Pe_r have a stronger propensity to orient in the direction of the walls. The action of the active rods is demonstrated to be hindered by translational diffusion, and for low translational Peclet numbers Pe_{perp}, the system resumes acting as in the case of the passive rods.
In simple shear flow, the presence of active rods causes shear banding, a divergence from the typical linear velocity profile. Rheological characteristics, viscosity, and normal stress differences alter when active rods' relative velocities and Peclet numbers increase. Additional research and testing are needed to validate and expand upon these findings. Future work will concentrate on studying the 3D cases in addition of expanding the rheological studies into more complex fluids.

V. SECOND-ORDER MOMENT OF Ψ

The second-order moment of Ψ, $\mathbf{A}_2$, contains information on the local concentration and orientation of particles and is defined as

$$\mathbf{A}_2 = \frac{1}{V}\int_{\mathbf{p}}\int_{\mathbf{r}_c} \mathbf{pp}\Psi d\mathbf{r}_c d\mathbf{p}. \tag{17}$$

The trace of $\mathbf{A}_2$ is the concentration field c, which represents the mean number density in the suspension, it is the zeroth-order moment of Ψ

$$c = \frac{1}{V}\int_{\mathbf{p}}\int_{\mathbf{r}_c} \Psi d\mathbf{r}_c d\mathbf{p}. \tag{18}$$

The first order moment of Ψ, $\mathbf{n}$, represents the nematic order of the particles and it is defined as

$$\mathbf{n} = \frac{1}{V}\int_{\mathbf{p}}\int_{\mathbf{r}_c} \mathbf{p}\Psi d\mathbf{r}_c d\mathbf{p}, \tag{19}$$

The third-order moment of Ψ, $\mathbf{A}_3$, is defined as

$$\mathbf{A}_3 = \frac{1}{V}\int_{\mathbf{p}}\int_{\mathbf{r}_c} \mathbf{ppp}\Psi d\mathbf{r}_c d\mathbf{p}, \tag{20}$$

while the fourth-order moment of Ψ, $\mathbf{A}_4$, is defined as

$$\mathbf{A}_4 = \frac{1}{V}\int_{\mathbf{p}}\int_{\mathbf{r}_c} \mathbf{pppp}\Psi d\mathbf{r}_c d\mathbf{p}. \tag{21}$$

The evolution equation of the concentration of the active particles in a suspending fluid is

$$\frac{Dc}{Dt} = D_\perp \nabla^2_{\mathbf{x}} c + (D_\parallel - D_\perp)\nabla_{\mathbf{x}}\nabla_{\mathbf{x}}\mathbf{A}_2 + V_s \nabla_{\mathbf{x}} \cdot (c\mathbf{n}) \tag{22}$$

V represents the volume, which is large enough to contain a statistically significant number of particles but smaller than the characteristic length scale of the macroscopic properties of the system under consideration. In the case of active particles, the odd-order tensors do not equal zeros due to the non-symmetric shapes of the particles. Since the active particles are not symmetric, unlike the passive particles, the orientation component A_{12}/c is not enough to give

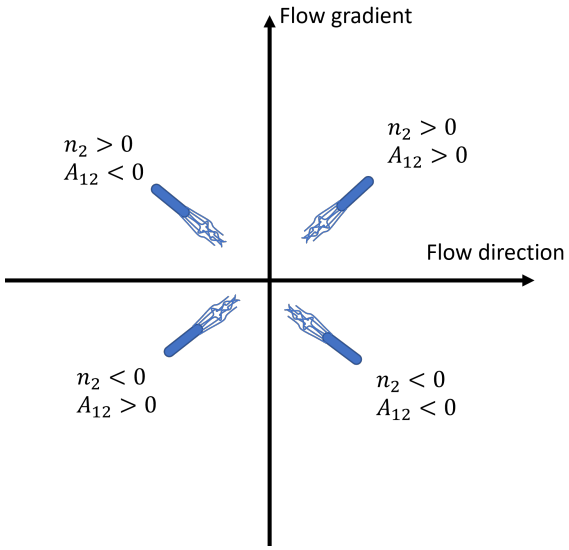

FIG. 9: Representation shows the meaning of the nematic order of a asymmetric particle.

information about the polarisation of the particle. Fig. 9 shows the different polarisation of the particle depending on the signs of A_{12} and n_2.
The evolution of $\mathbf{A}_2$ is obtained by premultiplying Eq. **??** with the tensor $\mathbf{pp}/V$ and integrating it over the spatial and configurational spaces.

$$\begin{aligned}\frac{D\mathbf{A}_2}{Dt} =& -\frac{1}{2}\left(\boldsymbol{\omega}\cdot\mathbf{A}_2 - \mathbf{A}_2\cdot\boldsymbol{\omega}\right) + \frac{\lambda}{2}\left(\dot{\boldsymbol{\gamma}}\cdot\mathbf{A}_2 + \mathbf{A}_2\cdot\dot{\boldsymbol{\gamma}} - 2\mathbf{A}_4 : \dot{\boldsymbol{\gamma}}\right) \\ &+ 2D_r\left(c\boldsymbol{\delta} - \alpha\mathbf{A}_2\right) + D_\perp\nabla^2_{\mathbf{x}}\mathbf{A}_2 + \left(D_\parallel - D_\perp\right)\nabla_{\mathbf{x}}\nabla_{\mathbf{x}} : \mathbf{A}_4 + V_s\nabla_{\mathbf{x}}\cdot\mathbf{A}_3.\end{aligned} \tag{23}$$

α equals 2 in 2D and 3 in 3D. It can be noticed that the time evolution of the tensor $\mathbf{A}_2$ depends on higher-order moments of Ψ. Hence, the problem requires a closure approximation. The last term in Eq. 23 is the Hessian operator and the last two terms of Eq. 23 implicitly show the coupling between the local concentration and the local orientation of Brownian particles. Unfortunately, unlike the case of passive particles, the closure approximations found in the literature do not work for non-symmetric particles. So the problem here requires closure approximations for solving $\mathbf{A}_4$ and $\mathbf{A}_3$ as a function of $\mathbf{A}_2$.

The derived macro-model enables one to solve a set of partial differential equations (PDEs) rather than a full 6D Fokker-Planck equation (Eq. **??**), to be discussed below, simplifying drastically the problem.

[1] ROTHSCHILD, Non-random distribution of bull spermatozoa in a drop of sperm suspension, Nature **198**, 1221 (1963).
[2] J. Hill, O. Kalkanci, J. L. McMurry, and H. Koser, Hydrodynamic surface interactions enable escherichia coli to seek efficient routes to swim upstream, Physical review letters **98**, 068101 (2007).
[3] A. P. Berke, L. Turner, H. C. Berg, and E. Lauga, Hydrodynamic attraction of swimming microorganisms by surfaces, Physical Review Letters **101**, 038102 (2008).
[4] E. Secchi, A. Vitale, G. L. Miño, V. Kantsler, L. Eberl, R. Rusconi, and R. Stocker, The effect of flow on swimming bacteria controls the initial colonization of curved surfaces, Nature communications **11**, 2851 (2020).
[5] J. P. Hernandez-Ortiz, C. G. Stoltz, and M. D. Graham, Transport and collective dynamics in suspensions of confined swimming particles, Physical review letters **95**, 204501 (2005).
[6] J. P. Hernandez-Ortiz, P. T. Underhill, and M. D. Graham, Dynamics of confined suspensions of swimming particles, Journal of Physics: Condensed Matter **21**, 204107 (2009).
[7] L. Vennamneni, S. Nambiar, and G. Subramanian, Shear-induced migration of microswimmers in pressure-driven channel flow, Journal of Fluid Mechanics **890**, A15 (2020).
[8] T. Kaya and H. Koser, Characterization of hydrodynamic surface interactions of escherichia coli cell bodies in shear flow, Physical review letters **103**, 138103 (2009).

[9] G. B. Jeffery, The motion of ellipsoidal particles immersed in a viscous fluid, Proceedings of the Royal Society of London. Series A, Containing papers of a mathematical and physical character **102**, 161 (1922).

[10] T. Kaya and H. Koser, Direct upstream motility in escherichia coli, Biophysical journal **102**, 1514 (2012).

[11] D. Saintillan and M. J. Shelley, Instabilities and pattern formation in active particle suspensions: kinetic theory and continuum simulations, Physical Review Letters **100**, 178103 (2008).

[12] D. Saintillan and M. J. Shelley, Instabilities, pattern formation, and mixing in active suspensions, Physics of Fluids **20** (2008).

[13] R. A. Simha and S. Ramaswamy, Hydrodynamic fluctuations and instabilities in ordered suspensions of self-propelled particles, Physical review letters **89**, 058101 (2002).

[14] Y. Hatwalne, S. Ramaswamy, M. Rao, and R. Aditi Simha, Rheology of active-particle suspensions, Phys Rev Lett **92**, 118101 (2004).

[15] T. Ishikawa and T. J. Pedley, The rheology of a semi-dilute suspension of swimming model micro-organisms, J Fluid Mech **588**, 399 (2007).

[16] B. M. Haines, I. S. Aranson, L. Berlyand, and D. A. Karpeev, Effective viscosity of dilute bacterial suspensions: a two-dimensional model, Phys Biol **5**, 1 (2008).

[17] D. Saintillan, The dilute rheology of swimming suspensions: A simple kinetic model, Experimental Mechanics **50**, 1275 (2010).

[18] H. M. López, J. Gachelin, C. Douarche, H. Auradou, and E. Clément, Turning bacteria suspensions into superfluids, Physical review letters **115**, 028301 (2015).

[19] S. Guo, D. Samanta, Y. Peng, X. Xu, and X. Cheng, Symmetric shear banding and swarming vortices in bacterial superfluids, Proceedings of the National Academy of Sciences **115**, 7212 (2018).

[20] L. Vennamneni, P. Garg, and G. Subramanian, Concentration banding instability of a sheared bacterial suspension, Journal of Fluid Mechanics **904**, A7 (2020).

[21] M. E. Cates and S. M. Fielding, Rheology of giant micelles, Adv. Phys. **55**, 799 (2006).

[22] P. D. Olmsted, Perspectives on shear banding in complex fluids, Rheol. Acta **47**, 283 (2008).

[23] T. Divoux, M. A. Fardin, S. Manneville, and S. Lerouge, Shear banding of complex fluids, Annu. Rev. Fluid Mech. **48**, 81 (2016).

[24] M. E. Cates, S. M. Fielding, D. Marenduzzo, E. Orlandini, and J. M. Yeomans, Shearing active gels close to the isotropic-nematic transition, Phys. Rev. Lett. **101**, 068102 (2008).

[25] A. Loisy, J. Eggers, and T. B. Liverpool, Active suspensions have nonmonotonic flow curves and multiple mechanical equilibria, Phys. Rev. Lett. **121**, 018001 (2018).

[26] M. Doi and S. Edwards, *The theory of polymer dynamics*, Vol. 73 (Oxford university press, 1988).

[27] H. Issa, G. Natale, G. Ausias, and J. Férec, Modeling and numerical simulations of brownian rodlike particles with anisotropic translational diffusion, Physical Review Fluids **8**, 033302 (2023).

[28] R. Alonso-Matilla, B. Ezhilan, and D. Saintillan, Microfluidic rheology of active particle suspensions: Kinetic theory, Biomicrofluidics **10** (2016).